



# Symmetrical indoor visible light layout optimized by a modified grey wolf algorithm

YIHANG ZUO,\*  BOJUN LIU, AND KUNMING SHAO

School of Micro-Electronics, South China University of Technology, Guangzhou, 511442, China

\*Corresponding author: 201965445107@mail.scut.edu.cn

Received 28 March 2022; revised 23 June 2022; accepted 26 June 2022; posted 27 June 2022; published 7 July 2022

**The indoor visible light communication system's LED layout and power factor affect the uniformity of the received power. To reduce the mean square error (MSE) of received power, a symmetrical optimization strategy based on the modified grey wolf optimization algorithm (mGWO) is proposed and applied in the square, rectangular, and circular rooms with different numbers of LED arrays. The received power uniformity, SNR uniformity, bit error rate, and channel capacity of the optimized layout with the proposed method are improved compared to the classical layout. The comparison results show that the mGWO can find the optimal layout efficiently.** © 2022 Optica Publishing Group

<https://doi.org/10.1364/AO.458919>

## 1. INTRODUCTION

Recently, the visible light communication (VLC) system based on the light-emitting diode (LED) has attracted extensive attention from researchers [1]. Unlike widely used wireless communication technology [2–5] (e.g., NFC, ZigBee, WiFi, 5G), VLC system's advantages include high power efficiency, wide bandwidth resources, high security, high flexibility, and fast deployment [6]. The indoor VLC system is a complementary technology to traditional RF wireless communication, composed of LED arrays placed on the ceiling and the receivers [7]. The LED arrays connect with the power line and information transmission line, which can simultaneously achieve illumination and signal transmission. The receiver analyzes and processes the received signal, which can realize the function of positioning and transmission [1].

In the whole system, the uniformity of the communication plane is an important indicator, which directly affects the communication quality and stability of the mobile receiver. However, due to the limitation of the inherent Lambert emission mode, the received power of a single LED decays rapidly from the center to the surrounding, and the communication quality of intelligent devices in different locations will be different [8]. More seriously, when there is a blind zone, the receiver will lose contact, and it may result in communication failure [9]. Therefore, it is of great significance to study the uniformity of optical power distribution on the communication plane.

In order to decrease the mean square error (MSE) of the received power, researchers have proposed many schemes and strategies. Ramane *et al.* [10] discussed the interdependencies of the source of luminous flux, spatial radiation distribution, geometry of the LED array, and source-to-target distance and analyzed the influence on the performance of VLC system.

Wang *et al.* [11] proposed a circular layout for a 16-lamp VLC system with the benefit of high signal-to-noise ratio (SNR), low bit error rate (BER), and high channel capacity, which indicates that changing the layout can improve the performance of indoor visible light systems. The authors in [12] transformed exploring the optimal LED position into a convex optimization problem and solved it with the Lagrange dual method. In [13], Varma *et al.* used a binomial point process to model the system and the golden section search algorithm to obtain the power distribution scheme. Manh Le Tran *et al.* [14] proposed a scheme that can achieve low received power variance and quality coefficient for power allocation and orientation through joint optimization. Su *et al.* [15] used the simulated annealing algorithm to achieve a good uniform illumination distribution on the target plane. Ding *et al.* determined a set of optimal power adjustment factors to make the received SNR distribution on the receiving plane more uniform to ensure the communication fairness of receivers at different positions in [16]. Pal [17] developed an optimization technique based on evolutionary programming to search for an optimal array structure. Liu [18] and Wang [19] used a gene density genetic algorithm and an improved artificial fish swarm algorithm to optimize the layout of 4-lamp and 16-lamp VLC systems, respectively, showing that lamp layout optimization could increase the uniformity of the received power. Furthermore, Wei *et al.* [20] improved the firefly algorithm for joint optimization of location, power allocation, and orientation of a LED lamp array. However, these algorithms usually need to be iterated thousands of times, which takes more than 10 h. Due to the limitation of the optimization strategy and algorithm, previous research results in multi-LED layout optimization still need some further improvement.

The contributions of this paper are as follows:

1. A new heuristic algorithm (mGWO) with high optimization speed is proposed.
2. A symmetrical optimization strategy is proposed and applied in rooms with different shapes.
3. The mGWO is compared with the algorithms of recent papers.

The rest of this paper is organized as follows. The system model and calculation process of the specifications for indoor VLC system are described in Section 2. Section 3 presents the modified grey wolf algorithm (mGWO) and describes the application process. In Section 4, the simulation results of asymmetric strategy and symmetric strategy are analyzed and compared with relative works. Section 5 shows the conclusions of this paper.

## 2. SYSTEM MODEL

As shown in Fig. 1, we build a 5 m × 5 m × 3 m indoor visible light system with all LED arrays placed on the ceiling. The position of the  $i$ th LED array is indicated as  $(x_i, y_i)$ , and one array has a 7 × 7 LED. The receiver is placed on the communication plane. The channel gain between the receiver and the LED array is related to their positions in space, which is generally calculated by the Lambertian radiation model [21,22] as Eq. (1),

$$H(0) = \begin{cases} \frac{(m+1)A}{2\pi D_d^2} \cos^m \varphi T_s(\phi)g(\phi) \cos \phi & 0 < \phi \leq \phi_c \\ 0 & \phi > \phi_c \end{cases}, \quad (1)$$

where  $A$  is the area of the receiver and  $D_d$  is the distance between the LED array and the receiver.  $m = \frac{-\ln 2}{\ln \cos \phi_{1/2}}$  is the Lambertian emission order, and  $\phi_{1/2}$  is semi-angle at half-power of the LED.  $\phi$  is the incident angle, and  $\varphi$  is the irradiation angle.  $\phi_c$  denotes the field of view (FOV) of the receiver.  $g(\phi)$  is the gain of condenser, which can be calculated by  $g(\phi) = \frac{n^2}{\sin^2 \phi_c}$ , and  $n$  denotes the refractive index of the lens at the photoelectric detector.

The received optical power of line-of-sight (LOS) links  $P_{LOS}$  can be derived with the channel gain and transmitted optical power  $P_t$ , as follows:

$$P_{LOS} = H(0) \cdot P_t. \quad (2)$$

In general, the received optical power  $P_r$  includes the power of LOS paths, the power of non-LOS (NLOS) paths, and background noise power,

$$P_r = P_{LOS} + P_{NLOS} + P_{Background}. \quad (3)$$

The core performance describing the uniformity of received power is the MSE, which is given as Eq. (4),

$$MSE = \sqrt{E\{[P_r - E(P_r)]^2\}}. \quad (4)$$

According to [23], the rate of the power to total power is 95.16% for the LOS link, 3.57% for the first reflection of NLOS link, and 1.27% for the second reflection. Since  $P_{NLOS}$  is affected by wall reflectivity, smoothness, and room shape, its value cannot be calculated accurately. On the other hand, for a practical application system, the values of  $P_{NLOS}$  are much smaller than  $P_{LOS}$  and can be regarded as noise power [24].

As in [13], the noise  $\sigma$  at the photoelectric detector consists of shot noise,  $\sigma_{shot}$ , and thermal noise,  $\sigma_{thermal}$ . The noise can be represented as

$$\sigma^2 = \sigma_{shot}^2 + \sigma_{thermal}^2, \quad (5)$$

where  $\sigma_{shot}$  is a first-order function of  $P_r$  and  $\sigma_{thermal}$  can be viewed as a constant.

The illumination intensity can be expressed as

$$I = I(0) \cos^m \varphi \cos \phi / D_d^2, \quad (6)$$

where  $I(0)$  is the luminous intensity of a LED. For evaluating the performance of illumination, we define the coverage rate (Cov), which can be written as

$$Cov = \frac{S_m}{S_{total}}, \quad (7)$$

where  $S_m$  is the area meeting illumination requirements and  $S_{total}$  is the total area of room. According to the international standard [25], the indoor illumination intensity  $I$  should be 300 lx ~ 1500 lx.

In general,  $\gamma = \rho^2 P_r^2 / \sigma^2$  is the received SNR, where  $\rho$  is the conversion efficiency of a PD. For the on-off keying (OOK) modulation scheme, the average BER,  $P_{BER}$ , can be expressed as [26]

$$P_{BER} = Q(\sqrt{\gamma}), \quad (8)$$

where  $Q(x) = \frac{1}{\sqrt{2\pi}} \int_x^\infty \exp(-\frac{y^2}{2}) dy$ . Since the value and fluctuation of BER is very small, we introduce  $B' = -\log_2 P_{BER}$  to represent the BER. When  $B' \geq 19.9$ , SNR is sufficient for keeping  $BER \leq 10^{-6}$  (using the OOK-NRZ modulation format).

According to Shannon's well-known formula, the channel capacity can be calculated as [26]–[28] (in bits/s/Hz)

$$C = \log_2(1 + \gamma). \quad (9)$$

In this paper, we use MSE as the objective function and utilize the average of received power, coverage rate, BER, and channel capacity to evaluate the indoor VLC system.

All variables used in this paper are summarized in Table 1.

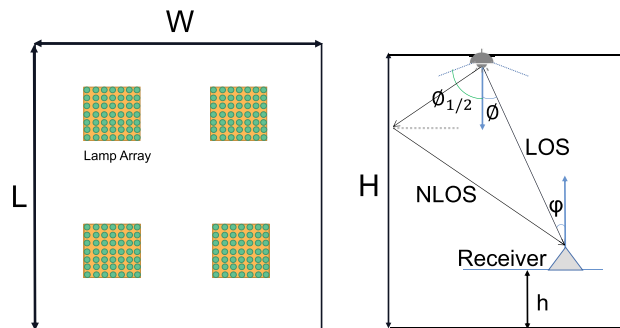


Fig. 1. Schematic diagram of system model.

**Table 1. Default Parameters in the Indoor VLC System**

Symbol	Parameters	Values
L * W * H	Room size	5 × 5 × 3 m
H	Height of communication plane	0.85 m
$P_t$	Transmitted power of a lamp	452 mW
$\phi_{1/2}$	Semi-angle at half-power	80 deg
	Number of LED in each array	7 × 7
$T_i(\phi)$	Gain of optical filter	1.0
$\phi_c$	Field of view (FOV)	55 deg
A	Physical area of the detector O/E	1.0 cm <sup>2</sup>
$\rho$	Conversion efficiency of a PD	0.53 A/W
N	Refractive index of lens at a PD	1.5
I(0)	Luminous intensity of a LED	23.81 cd

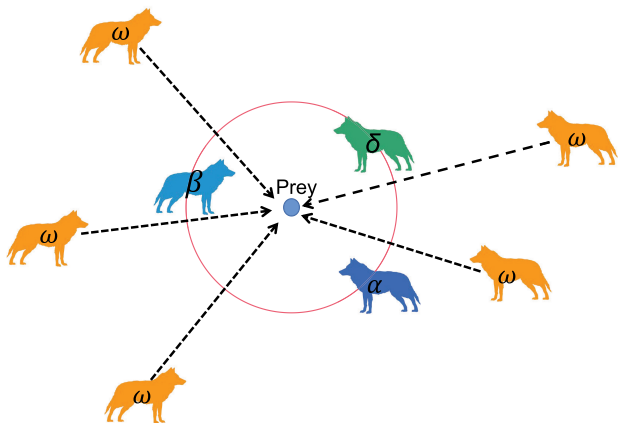
### 3. MODIFIED GREY WOLF OPTIMIZATION ALGORITHM

The grey wolf is considered to be apex predator, meaning that it is at the top of the food chain. According to their social structure and hunting strategy, Mirjalili [29] proposed a heuristic algorithm, the grey wolf optimization algorithm.

In order to mathematically model the social hierarchy of grey wolves, researchers consider the fittest solution as  $\alpha$ . In the same way, the second and third best solutions are named as  $\beta$  and  $\delta$ , respectively. The rest of the candidate solutions are assumed to be  $\omega$ . In the GWO algorithm, the hunting (optimization) is guided by  $\alpha$ ,  $\beta$ , and  $\delta$ . The  $\omega$  wolves follow other wolves, and their behaviors are shown as in Fig. 2.

In GWO, the process of searching for the optimal solution includes two parts: global exploration and local optimization, which is realized by gradually linear reducing the excessive parameter  $a$ . When  $a > 1$ , the wolves will jump out of the local optimum and conduct a global search. On the other hand, when  $a < 1$ , the wolves will focus on the local optimum. During the optimization of indoor visible light layout, more time needs to be spent in the global exploration due to high dimension solution space. Therefore, we propose a new nonlinear transition parameter  $a$  strategy, which can be expressed as

$$a = 2 \sin \left[ \left( 1 - \frac{t}{T} \right) \frac{\pi}{2} \right], \quad (10)$$

**Fig. 2.** Position updating in GWO.

where  $t$  is the current number of iterations and  $T$  is the total number of iterations.

In the original GWO, the position of prey is obtained by the averaging optimal positions of  $\alpha$ ,  $\beta$ , and  $\delta$  wolf. To make it more accurate, a modified weighted voting method is proposed here,

$$\vec{X}(t+1) = w_\alpha \cdot \vec{X}_\alpha + w_\beta \cdot \vec{X}_\beta + w_\delta \cdot \vec{X}_\delta, \quad (11)$$

where  $\vec{X}_\alpha$  is the position vector of the  $\alpha$  prey and  $\vec{X}(t+1)$  indicates the position at  $t+1$  iteration.  $w_\alpha$ ,  $w_\beta$ ,  $w_\delta$  replace the decision weight of  $\alpha$ ,  $\beta$ , and  $\delta$  during hunting, which is calculated by Eq. (12).  $F_i$  indicates the fitness value of a different grey wolf, where  $i = \alpha, \beta, \delta$ ,

$$w_i = \frac{\frac{1}{F_i}}{\frac{1}{F_\alpha} + \frac{1}{F_\beta} + \frac{1}{F_\delta}}. \quad (12)$$

The reverse learning strategy is an intelligent algorithm optimization strategy proposed by Tizooosh [30] in 2005 to improve the search performance. Similar to the  $\alpha$ ,  $\beta$ , and  $\delta$  wolf, the information of the worst wolves in the wolves is also a representative of the knowledge and experience accumulated by the current wolves. For individuals with poor fitness, it is more efficient to reverse their position in the solution space instead of moving toward the target position. The process can be written as

$$x^* = a_j + b_j - x, \quad (13)$$

where  $a_j$  and  $b_j$  represent the upper and lower boundary of the search space, respectively, and  $x$  is the position of wolf.

For the VLC system layout with  $i$  LED arrays, Position[ $X_1, Y_1, P_1, X_2, Y_2, P_2, \dots, X_i, Y_i, P_i$ ], is the target that needs to be optimized. ( $X_i, Y_i, P_i$ ) is the position and power factor of the  $i$ th LED array, which is also used as the position of the wolf. In general, ( $X_i, Y_i$ ) is the position in the rectangular coordinate system, and it will be rewritten as ( $R_i, \theta_i$ ) in polar coordinates in circular zooms. The orientation can be written as

$$\min \text{MSE} = \text{fitness}(P), \quad (14)$$

$$\begin{aligned} \text{s.t. } & \text{Lowerboundary} \leq X \text{ or } R \leq \text{Upperboundary} \\ & \text{Lowerboundary} \leq Y \text{ or } \theta \leq \text{Upperboundary} \\ & P_t - 0.5P_t \leq P \leq P_t + 0.5P_t \end{aligned} \quad (15)$$

The pseudo code of the mGWO algorithm is shown in Algorithm 1.

### 4. RESULTS AND DISCUSSION

In this section, simulations are conducted, and corresponding results are analyzed. First, for the classical 4 LED layout (square layout) and 16 LED layout (rectangular layout), the effect of power, location, and L + P optimization are evaluated. Then, we propose and apply the symmetric optimization strategy to square, rectangular, and circular rooms. Finally, the mGWO is compared with relative works.

**Algorithm 1. Modified Grey Wolf Optimizer Algorithm**

**Input:** Array number, iteration number, population number.

**Output:** Optimal solution, fitness curve

- 1: Random initialize wolf position
- 2: **for**  $i = 1; i < iteration\ number; i + +$  **do**
- 3: Check boundary conditions
- 4: Calculate the fitness (MSE) of each wolf
- 5: **for** Each wolf **do**
- 6: **if** Fitness is the last three **then**
- 7: Reverse position
- 8: **else**
- 9: Update position

**A. Asymmetric Optimization**

The square layout of four LED arrays is a widely used VLC system layout as shown in Fig. 1. We implement location optimization (L), power optimization (P), and joint optimization (L + P), which are compared with the square layout (S). The received power distribution is presented in Figs. 3(a)–3(d).

Table 2 shows the detailed indicators with four different layouts.  $\bar{P}$  indicates the average received power, which is positively correlated with SNR when the noise is approximately unchanged. Optimizing the location alone can effectively reduce MSE, but BER, Cov, and channel capacity will also decrease, which will lead to poor communication performance. SNR and Cov both increase when optimizing the power solely, but MSE does not decrease. Single degree of freedom optimization cannot achieve good performance in all respects. Only the double degree of freedom optimization, joint optimization can reduce MSE and increase others at the same time.

Figure 4 is the power distribution diagram of the VLC system with 16 LED arrays in various cases. Compared with the rectangular layout (R), the optimized power distribution is flatter, but the SNR is reduced. The indicators of various layouts are illustrated in Table 3. The power optimization layout has less loss on the communication performance than location optimization, but location optimization can more effectively improve the uniformity of the received power. Circular layout (C) is a

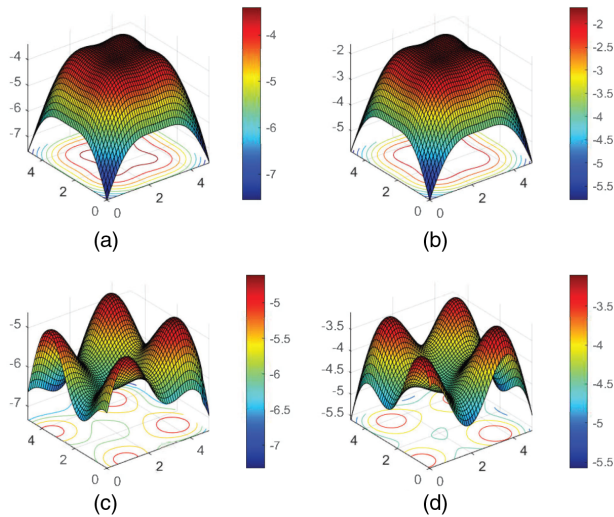


**Fig. 3.** Received power of four LED arrays. (a) Square layout, (b) power optimization, (c) location optimization, and (d) L + P optimization.

**Table 2.** Performance of VLC Systems with Four LED Arrays

Layout	$\bar{P}$ (dBm)	MSE (dBm)	Cov	$B'$	C (bits/s/Hz)
S	-4.46	0.93	70.0%	37.96	5.64
L	-5.63	0.49	9.76%	36.26	5.57
P	-2.70	0.93	97.6%	40.51	5.73
L + P	-4.05	0.44	98.24%	38.56	5.66

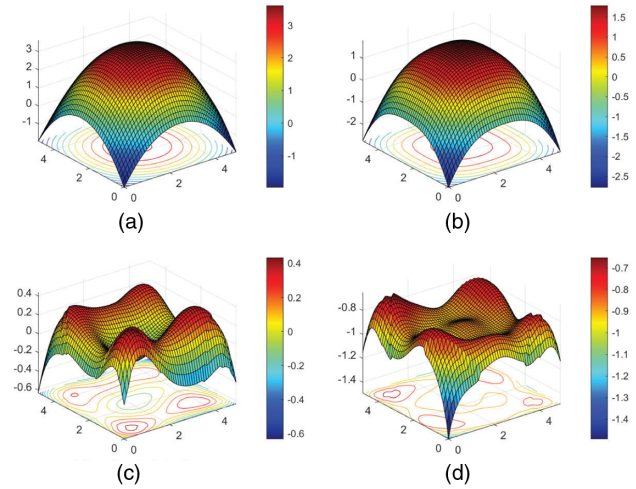


**Fig. 4.** Received power of 16 LED arrays. (a) Rectangle layout, (b) power optimization, (c) location optimization, and (d) L + P optimization.

classical layout proposed in [11], which is widely used in VLC systems with 16 lamps. L optimization and L + P optimization have comprehensive advantages over circular layout. For L + P optimization, MSE will decrease more than other optimization methods. However, these three methods will significantly reduce  $\bar{P}$  (SNR), which is crucial to the performance of VLC systems.

The VLC system layout after L + P optimization is shown in Fig. 5. The layout has a high degree of symmetry. In order to get a general rule, we obtain the layout after L + P optimization with different numbers of LED arrays, which is illustrated in Fig. 6. It seems that the optimal layout has a certain degree of symmetry, which is the same as [20].

**B. Symmetric Optimization**

Since there are four axes of symmetry for the square rooms, we can divide the space into eight zones, as is shown in Fig. 5.

Since all the areas are symmetrical with the adjacent area, the layout designed for any one of them can be copied to the others

**Table 3.** Performance of VLC Systems with 16 LED Arrays

Layout	$\bar{P}$ (dBm)	MSE (dBm)	Cov	$B'$	C (bits/s/Hz)
R	1.66	1.26	57.6%	46.71	5.94
L	-0.53	0.14	100%	43.63	5.84
P	0.34	1.01	100%	44.86	5.89
C [11]	-1.06	0.29	100%	42.87	5.82
L + P	-0.87	0.09	100%	43.13	5.83

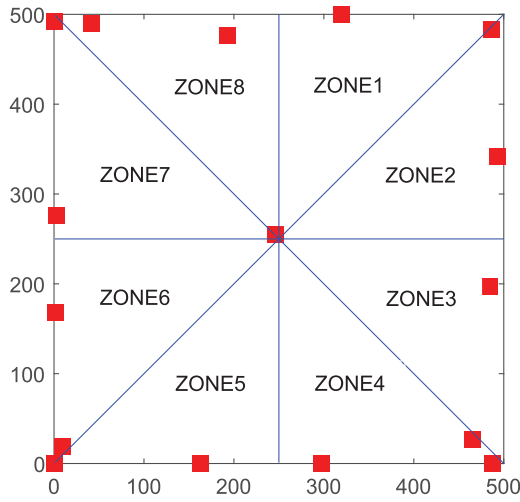


Fig. 5. Sixteen LED layout after L + P optimization.

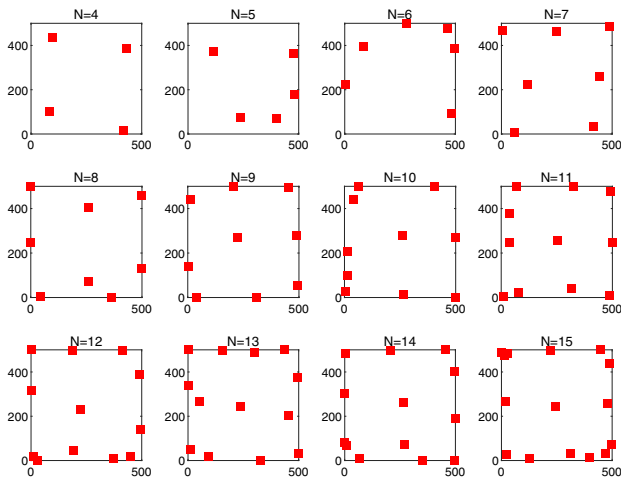


Fig. 6. Layout with 4–15 LED arrays.

symmetrically. In general, we need place one or two lamps in every zone, so two cases need to be considered: 8 lamps and 16 lamps. Particularly, combined with the experimental results in Section 4.A, we also study the cases of 9 LED arrays and 17 LED arrays with one additional lamp pre-placed in the center of the room. The power of lamps at the corresponding position is the same except for the pre-placed lamp.

For 16 LED arrays, two lamps are placed in each zone. The target that needs to be optimized can be presented as  $[X_1, Y_1, P_1, X_2, Y_2, P_2]$ , which decreases from 48 dimensions to 6 dimensions. The solution space is compressed to one-eighth of the original. As for 17 LED arrays, it only requires an additional power factor, and its target is  $[X_1, Y_1, P_1, X_2, Y_2, P_2, P_3]$ .

The optimized LED layout is shown in Fig. 7. For the 17 LED array system, two lamps are placed at the same position (the middle point of each side). Therefore, only 13 LED arrays can be observed in the layout.

Comparing the results shown in Table 4, it can be found that the symmetrical layout with 16 or 17 lamps has advantages in SNR and communication indicators. The pre-placed layout, 9 LED layout, is better than the 8 LED layout on all indicators. In the 16 LED array system, the MSE of the symmetrical layout

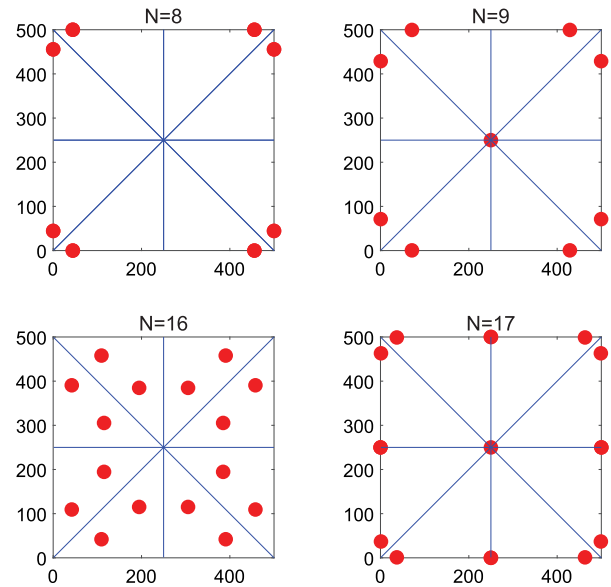


Fig. 7. Symmetric layout in a square room.

Table 4. Performance of a Square Room

	$\bar{P}$ (dBm)	MSE (dBm)	Cov	$B'$	C (bits/s/Hz)
8 lamps	-1.98	0.85	2%	37.88	5.63
9 lamps	-0.64	0.41	48%	41.5	5.77
16 lamps	3.34	0.76	22.72%	49.04	6.01
17 lamps	1.57	0.07	100%	46.60	5.94

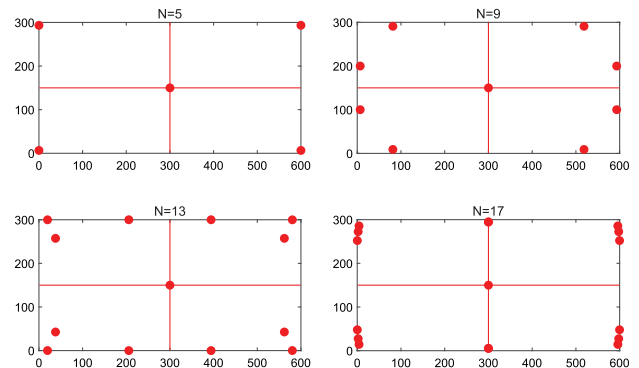


Fig. 8. Symmetric layout in a rectangular room.

reduces 39.7% compared with the rectangular layout, and the average received power increases 101%. The channel capacity is also higher than the rectangular layout. After pre-placing a LED array in the center of the room, the MSE will be reduced to 0.07, less than the MSE of the layout obtained through L + P optimization. The average power and the communication performance of the symmetric 17 lamp layout are better than the L + P optimization layout.

For the rectangular room, the symmetric optimization strategy is still applicable. For a 6 m × 3 m rectangular room, it can be divided into four zones by two axes of symmetry. Due to FOV, the coverage of each LED array is limited, so a LED array must be pre-placed in the center of the room to avoid the received power being 0 during the optimization process.

**Table 5. Performance of a Rectangular Room**

	$\bar{P}$ (dBm)	MSE (dBm)	Cov	$B'$	$C$ (bits/s/Hz)
5 lamps	-6.31	0.50	100%	35.25	5.52
9 lamps	-4.19	0.40	100%	38.36	5.65
13 lamps	-2.94	0.15	100%	40.16	5.72
17 lamps	-2.75	0.22	100%	40.44	5.73

Figure 8 presents the layout with 5, 9, 13, and 17 LED arrays. Table 5 illustrates detailed indicators about Fig. 8.

With the increase of the LED array number, the average power increases from -6.31 dbm to -2.75 dbm. The  $B'$  of the system increases from 35.25 to 40.44, and the channel capacity increases from 5.52 bits/s/Hz to 5.73 bits/s/Hz. The above shows that the communication performance of the VLC system is directly proportional to the number of lamps. The layout with 13 lamps has the lowest, which has the best uniformity of the received power, followed by the 17 LED array system.

The circle has an infinite number of axes of symmetry, which can be used for further research. For a circular room with a radius equal to 2.5 m, we divide this room into  $N$  parts equally, and each part has a LED array. For the LED array in part 1, the position in the polar coordinates constraint condition of the LED is as Eq. (16),

$$[0, 0] \leq [r, \theta] \leq \left[ 2.5, \frac{360^\circ}{N} \right]. \quad (16)$$

The position of other LED arrays can be obtained by rotating the position of the first array. The position of the  $i$ th LED array is  $[r, \theta + \frac{360^\circ}{N} \times (i - 1)]$ .

Another consideration is to pre-place a LED array in the center of the room. We optimize the location and power factor in two cases and obtain the curves as shown in Fig. 9.

In both curves, MSE will decrease significantly with the increase of the LED array's number. In two cases, the MSE of the pre-placed layout is smaller than that of the non pre-placed layout. The average power without pre-placed layout is increasing on the whole, but it will decrease in some cases, which is different from the average power of the pre-placed layout. Two curves begin to coincide after the number of LED arrays is larger than a critical value ( $N$  is greater than 13). With the increase of the number, the pre-placed lamp will lead to the illumination intensity exceeding the upper boundary of the international standard, so the coverage rate will decrease. In summary, the performance of the non pre-placed layout is better than the pre-placed layout when the LED number is 15 or 16, while the pre-placed layout has better performance when the number is 5 or 6.

**C. Performance Comparison of Other Algorithms**

In order to measure the performance of the mGWO algorithm, a variety of algorithms are compared with the mGWO on different test benchmarks. First, we compare the GDGA [8], IAFSA [19], and mGWO algorithm under the optimization of 16 LED arrays. Then, the FA [20], GWO algorithm [29], and mGWO are compared on optimizing symmetrical layout with 17 LED arrays. The population is 50, and other parameters are consistent with these papers. The results are shown in Fig. 10.

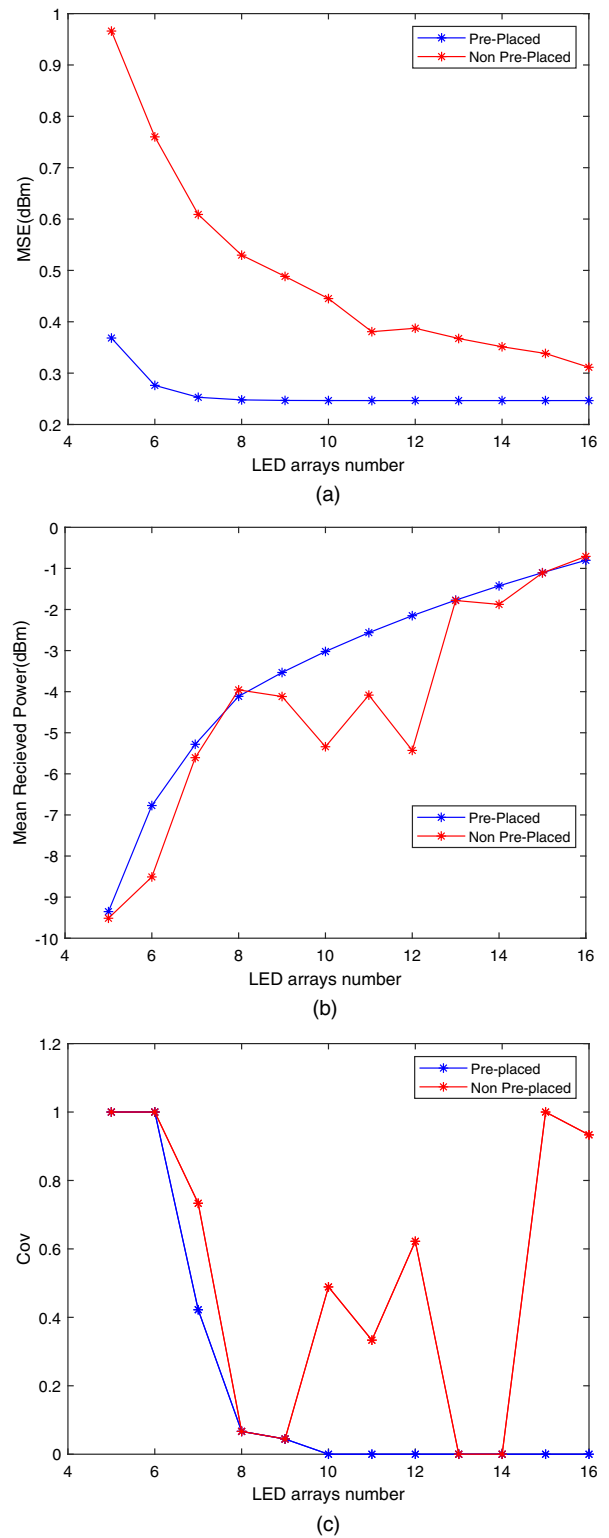


**Fig. 9.** Performance of a symmetric layout in a circular room. (a) MSE, (b) mean received power, and (c) coverage rate.

In Fig. 10, as the iteration number increases, the root MSE of the system gradually decreases. Compared with the GDGA algorithm and IAFSA algorithm, the mGWO algorithm decreases faster. GDGA and IAFSA do not decline after the 10th generation, trapped in the local optimal solution. In the

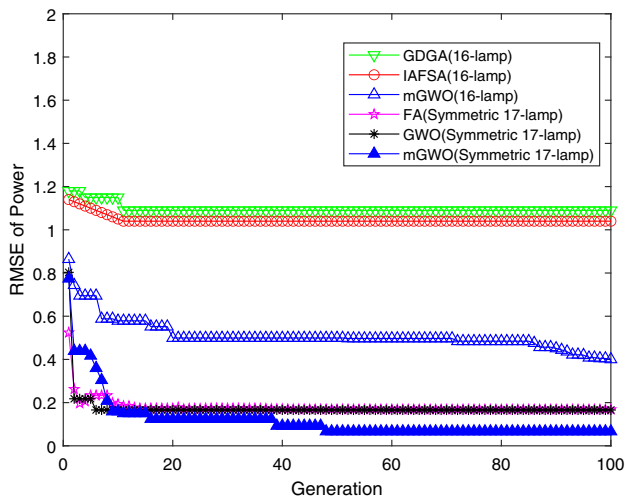


**Fig. 10.** Iteration curves.

optimization of symmetry layout with 17 LED arrays, mGWO also shows some advantages. Compared with the recent swarm intelligence algorithm, FA, and the original GWO algorithm, mGWO is more potent in global exploration, so it is easier to find the optimal solution.

## 5. CONCLUSION

This paper proposes a mGWO in order to optimize VLC system layout, which has a higher probability to jump out of the local optimal solution. After analyzing the optimization results of asymmetric optimization by mGWO, a symmetric optimization strategy is proposed, which can reduce the fluctuation of received power. The superiority of this strategy is proved in the experiment of square, rectangular, and circular rooms. The performance of results also shows that the strategy has advantages of low BER, large channel capacity, and easy realization. The comparison results show that mGWO is a high efficient heuristic algorithm.

**Disclosures.** The authors declare no conflicts of interest.

**Data availability.** Data underlying the results presented in this paper are not publicly available at this time but may be obtained from the authors upon reasonable request.

## REFERENCES

- P. H. Pathak, X. Feng, P. Hu, and P. Mohapatra, "Visible light communication, networking, and sensing: a survey, potential and challenges," *Commun. Surveys Tuts.* **17**, 2047–2077 (2015).
- R. Want, "Near field communication," *IEEE Pervasive Comput.* **10**, 4–7 (2011).
- K. Gill, S.-H. Yang, F. Yao, and X. Lu, "A ZigBee-based home automation system," *IEEE Trans. Consum. Electron.* **55**, 422–430 (2009).
- Y. He, M. Chen, B. Ge, and M. Guizani, "On WiFi offloading in heterogeneous networks: various incentives and trade-off strategies," *Commun. Surveys Tuts.* **18**, 2345–2385 (2016).
- K. Shafique, B. A. Khawaja, F. Sabir, S. Qazi, and M. Mustaqim, "Internet of things (IoT) for next-generation smart systems: a review of current challenges, future trends and prospects for emerging 5G-IoT scenarios," *IEEE Access* **8**, 23022–23040 (2020).
- W. Yan, "The study of indoor wireless communication technology based on LED," Ph.D. thesis (Taiyuan University of Technology, 2011).

- Y. Tanaka, T. Komine, S. Haruyama, and M. Nakagawa, "Indoor visible light data transmission system utilizing white LED lights," *IEICE Trans. Commun.* **E86B**, 2440–2454 (2003).
- H. Liu, P. Xia, Y. Chen, and L. Wu, "Interference graph-based dynamic frequency reuse in optical attocell networks," *Opt. Commun.* **402**, 527–534 (2017).
- A. M. Ramirez-Aguilera, J. M. Luna-Rivera, R. Perez-Jimenez, J. Rabadan-Borges, V. Guerra, and C. Suarez-Rodriguez, "Visible light communication constraints in practical indoor lighting systems," in *22th European Wireless Conference* (2016), pp. 1–5.
- D. Ramane and A. Shaligram, "Optimization of multi-element LED source for uniform illumination of plane surface," *Opt. Express* **19**, A639–A648 (2011).
- Z. Wang, C. Yu, W.-D. Zhong, J. Chen, and W. Chen, "Performance of a novel LED lamp arrangement to reduce SNR fluctuation for multi-user visible light communication systems," *Opt. Express* **20**, 4564–4573 (2012).
- Y. Yang, Z. Zhu, C. Guo, and C. Feng, "Power efficient LED placement algorithm for indoor visible light communication," *Opt. Express* **28**, 36389–36402 (2020).
- G. V. S. S. P. Varma, R. Sushma, V. Sharma, A. Kumar, and G. V. V. Sharma, "Power allocation for uniform illumination with stochastic LED arrays," *Opt. Express* **25**, 8659–8669 (2017).
- M. L. Tran and S. Kim, "Joint power allocation and orientation for uniform illuminance in indoor visible light communication," *Opt. Express* **27**, 28575–28587 (2019).
- Z. Su, D. Xue, and Z. Ji, "Designing LED array for uniform illumination distribution by simulated annealing algorithm," *Opt. Express* **20**, A843–A855 (2012).
- J. Ding, Z. Huang, and Y. Ji, "Evolutionary algorithm based power coverage optimization for visible light communications," *IEEE Commun. Lett.* **16**, 439–441 (2012).
- S. Pal, "Optimization of LED array for uniform illumination over a target plane by evolutionary programming," *Appl. Opt.* **54**, 8221–8227 (2015).
- H. Liu, X. Wang, Y. Chen, D. Kong, and P. Xia, "Optimization lighting layout based on gene density improved genetic algorithm for indoor visible light communications," *Opt. Commun.* **390**, 76–81 (2017).
- W. Jiaan, X. Ancheng, J. Jintao, and G. Linyang, "Optimization lighting layout of indoor visible light communication system based on improved artificial fish swarm algorithm," *J. Opt.* **22**, 035701 (2020).
- Z. Wei, H. Hu, and H. Huang, "Optimization of location, power allocation and orientation for lighting lamps in a visible light communication system using the firefly algorithm," *Opt. Express* **29**, 8796–8808 (2021).
- A. P. Tang, J. M. Kahn, and K.-P. Ho, "Wireless infrared communication links using multi-beam transmitters and imaging receivers," in *International Conference on Communications (ICC/SUPERCOMM)* (IEEE, 1996), Vol. 1, pp. 180–186.
- F. R. Gfeller and U. Bapst, "Wireless in-house data communication via diffuse infrared radiation," *Proc. IEEE* **67**, 1474–1486 (1979).
- J. R. Barry, *Wireless Infrared Communications* (Springer, 1994), Vol. **280**.
- L. Huang, P. Wang, Z. Liu, X. Nan, L. Jiao, and L. Guo, "Indoor three-dimensional high-precision positioning system with bat algorithm based on visible light communication," *Appl. Opt.* **58**, 2226–2234 (2019).
- "Lighting standard EN12464-1-FAGERHULT (international)," (2016).
- R. Sharma, M. Aggarwal, and S. Ahuja, "Channel capacity and BER estimation of indoor optical wireless communication system under receiver mobility," *J. Opt. Commun.* **39**, 413–426 (2018).
- C. E. Shannon, "A mathematical theory of communication," *Bell Syst. Tech. J.* **27**, 379–423 (1948).
- C. E. Shannon, "Communication in the presence of noise," *Proc. IRE* **37**, 10–21 (1949).
- S. Mirjalili, S. M. Mirjalili, and A. Lewis, "Grey wolf optimizer," *Adv. Eng. Softw.* **69**, 46–61 (2014).
- H. R. Tizhoosh, "Opposition-based learning: a new scheme for machine intelligence," in *International Conference on Computational Intelligence for Modelling, Control and Automation and International Conference on Intelligent Agents, Web Technologies and Internet Commerce (CIMCA-IAWTIC)* (IEEE, 2005), Vol. 1, pp. 695–701.